Computed Phase Equilibria and Material Studies for the Zirconia – Gadolinia – Dysprosia - Yttria System

E. C. Corcoran

Supervisors: W. T. Thompson and B. J. Lewis

Chemical and Materials Engineering in the Department of Chemistry and Chemical Engineering,
Royal Military College of Canada,
P. O. Box 17000, St. Forces, Kingston, Ont., Canada K7K 7B4
Phone: 613-541-6000 ext. 6510, Fax: 613-545-8341, email: emily.corcoran@rmc.ca

Abstract - Neutron absorbing elements are required in the center of advanced CANDU fuel bundle designs that make use of slightly enriched uranium in the surrounding elements. Dysprosia mixed with uranium dioxide is one such absorber that has been used for Low Void Reactivity Fuel (LVRF)[1]. An inert zirconia (with and without yttria) mixture is also being considered as a carrier for the neutron absorbers gadolinium and dysprosium. This quaternary oxide system was modeled from the binary oxide phase diagrams involving zirconia using interpolation methods to estimate the Gibbs energies of the multi-component phases. The model provides the solubility of Ln_2O_3 (Ln=Y,Gd,Dy) in the cubic structure of ZrO_2 as well as the temperature where the cubic phase is expected to melt or decompose into more stable solid phases.

1 Introduction

Fundamental thermodynamics can be applied to determine the most stable phases at specific conditions of composition and temperature [2]. This capability is especially useful at high temperature where experimental work is difficult to conduct. This paper provides a computed phase diagram for a proposed new material for the central element of a CANDU fuel bundle which contains zirconia (ZrO_2), and a mixture of yttria (Y_2O_3), gadolinia (Gd_2O_3), and dysprosia (Dy_2O_3) [1]. The central element does not provide fissionable material but rather is intended to capture neutrons to reduce coolant void reactivity when slightly enriched uranium oxide is used in the surrounding fuel elements.

The project first involved modelling the binary phase diagram using equations to represent the Gibbs energy of the phases as a function of composition and temperature for zirconia-gadolinia, zirconia-dysprosia and zirconia-yttria systems. Thereafter these thermodynamic models were combined using an interpolation scheme to generate the quaternary system.

2 Rare Earth Oxides (REO)

Dysprosium and gadolinium are members of the rare earth or lanthanide series of elements ($57 \leq$ Atomic No. ≤ 71). Another member of Group 3B, yttrium (Y, Atomic No. 39) is usually also included in discussing lanthanide chemistry. For simplicity, Ln will be used to represent all of the chemically similar lanthanide elements (La to Lu and Y). Those in this series are characterized by small chemical distinctions that stem from the partially filled 4f electron orbital. Yttrium has no "f" electron but has a similar ionic radius (Ln^{3+}) to other "true" lanthanides and generally similar chemistry as well [3].

The 3^+ oxidation state leads to the formation of the very stable Ln_2O_3 referred to as a sesquioxide. Depending on the ionic radius, sesquioxides generally crystallize into three main structures namely: hexagonal, monoclinic, and cubic [3]. The cubic structure bears many similarities to cubic zirconia.

3 Modelling Mixed Oxide Systems

When modelling an oxide solid solution, it is important to keep in mind that the cations (Zr^{4+} and Ln^{3+}) interchange on similar sites within a continuous lattice of oxide ions. This reality is best remembered by selecting as the formula mass of the lanthanide oxides $LnO_{1.5}$ rather than Ln_2O_3 so that a mole of each oxide component contributes the same number of moles of cations to the solid solution. The cubic solid solution of ZrO_2 and $LnO_{1.5}$ provides a good basis for discussion on this subject.

4 Crystal Structure of Cubic ZrO_2 and Cubic Ln_2O_3

4.1 Cubic ZrO_2

Zirconium oxide (like UO_2) is isomorphous with mineral CaF_2 (fluorite) as shown in Figure 1.

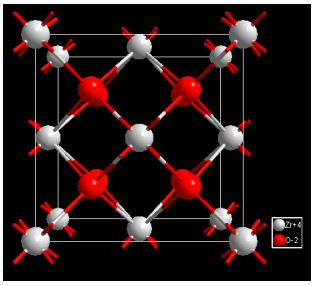


Figure 1. The cubic (fluorite) structure of ZrO_2. White atoms represent Zr^{4+} ions; red atoms represent O^{2-} ions [4].

Chemically, the actual unit cell contains 12 complete atoms (ions). In each unit cell there are eight O^{2-} ions, eight Zr^{4+}, 1/8th corner atoms, and six Zr^{4+} 1/2 atoms on each face (Zr_4O_8). This structure can be represented by the Pearson symbol of cF12 [5] or more uniquely by the Hermann-Maugin space group symbolism, Fm-3m [6].

4.2 Cubic Ln_2O_3 (C-type structure)

In cubic Ln_2O_3, the Ln^{3+} ions have similar radii as the Zr^{4+} ions, and form a similar fluorite-like arrangement as ZrO_2 provided the temperature is not too high. To maintain charge neutrality, one quarter of the oxide ion sites are vacant. These vacancies appear in a three-dimensional periodic pattern which distorts the placement of oxide ions as in fluorite [3]. This is shown on the left side of Figure 2 in which the true unit cell is difficult to visualize. Therefore, one-eighth of this unit cell is shown in the right side of Figure 2 where it is evident that only six O^{2-} ions (red) surround the Ln^{3+} ions (white). It is this side of Figure 2 that bears close comparison with Figure 1.

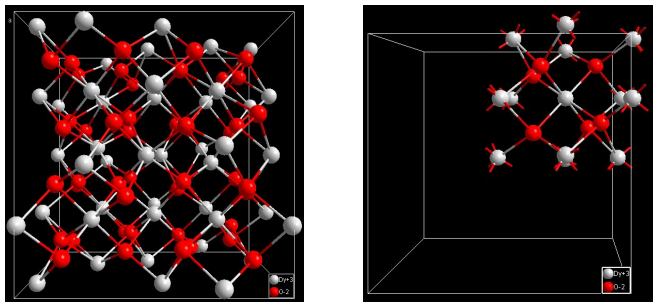


Figure 2. Bixbyite structure of gadolinium oxide. Complete cF80 unit cell (left). 1/8th of the unit cell (right). White atoms represent Gd^{3+} ions; red atoms represent O^{2-} ions. Note: the distortion of the oxide plane (as compared to Figure 1) is caused by the absence of O^{2-} ion[4].

The Pearson Symbol for cubic Ln_2O_3 is cF80 (32 Gd^{3+} ions + 48 O^{2-} ions). The Hermann-Maugin space group is Ia-3. These notational practices relay the otherwise close structural similarities of cubic ZrO_2 and cubic Ln_2O_3.

5 Mixing Oxides to Form Solid Solutions

When cubic solid oxide solutions of ZrO_2 and Ln_2O_3 are formed, the Zr^{4+} and Ln^{3+} ions interchange on cation lattice sites. The difference in charge affects the number and placement of vacancies throughout the crystal structure. This has a direct (although small) effect on the Gibbs energy of the system which affects the thermodynamic stabilities of the cubic solid solution relative to other potential phases at comparable conditions of temperature (and pressure).

As mentioned above, it is convenient to select the formula mass of the lanthanide sesquioxide as $LnO_{1.5}$. This formula mass contains 1 mol of cations as does the formula mass for zirconia, ZrO_2. Because of the potential confusion in representing composition, computed binary phase diagrams include three scales: mole fraction (X) of ZrO_2-$LnO_{1.5}$, mole fraction ZrO_2-Ln_2O_3, and weight percent (*wt%*) lanthanide oxide. A conversion table for zirconia-gadolinia mixtures is shown in Table 1 below. Note that the formula mass selected for the lanthanide sesquioxide has numerical affects on what is meant by the mole fraction of ZrO_2.

Table 1. Conversion table between the three compositional scales in the zirconia-gadolinia system.

wt% Gadolinia	$X_{GdO_{1.5}}$	X_{ZrO_2}	$X_{Gd_2O_3}$	X'_{ZrO_2}
0	0	1	0	1
26.9	0.2	0.8	0.11	0.89
49.5	0.4	0.6	0.25	0.75
68.8	0.6	0.4	0.42	0.58
85.5	0.8	0.2	0.66	0.44
100	1	0	1	0

6 Binary Systems

Phase diagrams are maps of the most stable phase(s) as a function of composition and temperature. The hydrostatic pressure is set at 1 atm although this variable is of little consequence unless the variation is extreme (several kbars). To illustrate the fundamentals of the subject matter [7], ZrO_2-$GdO_{1.5}$ will be examined at 2500°C where for simplicity only the relative stability of the cubic and liquid phases is considered.

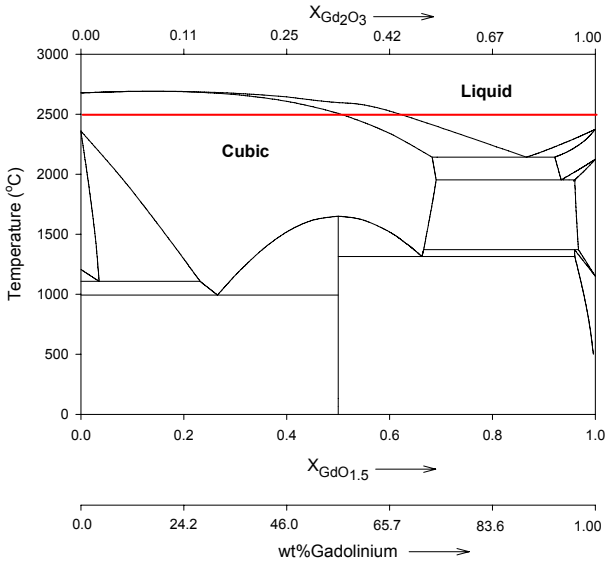


Figure 3. Binary phase diagram for ZrO_2 and $GdO_{1.5}$. Red line highlights the isotherm at 2500°C.

The phase(s) may be determined by the process of Gibbs energy minimization. The phase(s) present at a given temperature and overall composition must provide the lowest Gibbs energy (G) for the system as a whole. For a binary isobaric system, the change in Gibbs resultant from mixing (dissolution) may be viewed as the summation of an ideal mixing term (ΔG_{ideal}) and an excess Gibbs energy term (G^E) [2]:

$$\Delta G_{mix} = \Delta G_{ideal} + G^E \tag{1}$$

The ideal mixing term assumes cations [Zr^{4+}, Gd^{3+}] in the binary system randomly interchange on similar lattice sites. For one mole of solution the ideal mixing may be represented by [2]:

$$X_{ZrO_2} ZrO_2 + X_{GdO_{1.5}} GdO_{1.5} = (ZrO_2 - GdO_{1.5})_{Solution} \tag{2}$$

The ideal Gibbs energy of mixing for this process based on the assumption of random mixing of the cations is closely represented by [2]:

$$\Delta G_{ideal} = X_{ZrO_2} RT \ln X_{ZrO_2} + X_{GdO_{1.5}} RT \ln X_{GdO_{1.5}} \tag{3}$$

where X_{ZrO_2} and $X_{GdO_{1.5}}$ are the mole fractions of ZrO_2 and $GdO_{1.5}$, respectively, R is the ideal gas constant, and T is the absolute temperature (K). The ideal mixing term overlooks the thermal effects associated with mixing. To adjust the Gibbs energy for any departure from the ideal term, an excess (G^E) term is added. The excess Gibbs energy may be represented as an empirical series [2]:

$$G^E = X_{ZrO_2} X_{GdO_{1.5}} (p_o + p_1 X_{GdO_{1.5}} + p_2 X^2_{GdO_{1.5}} + \ldots) \quad (4)$$

where the coefficients of p may be functions of temperature (often linear). To simplify, the empirical series in Equation 4 can be truncated to:

$$G^E = p_o X_{ZrO_2} X_{GdO_{1.5}} \quad (5)$$

where p_o is a constant. These are called "regular" solutions [2]. The Gibbs energy curves can be constructed for the cubic and liquid phases at 2500°C and 1 atm as functions of $X_{GdO_{1.5}}$ with an appropriate value of p_o for each phase. Combined with a knowledge of the Gibbs energy difference between the cubic and liquid phases of the pure component oxides, the Gibbs energy curves for the cubic and liquid phases appear as shown in Figure 4.

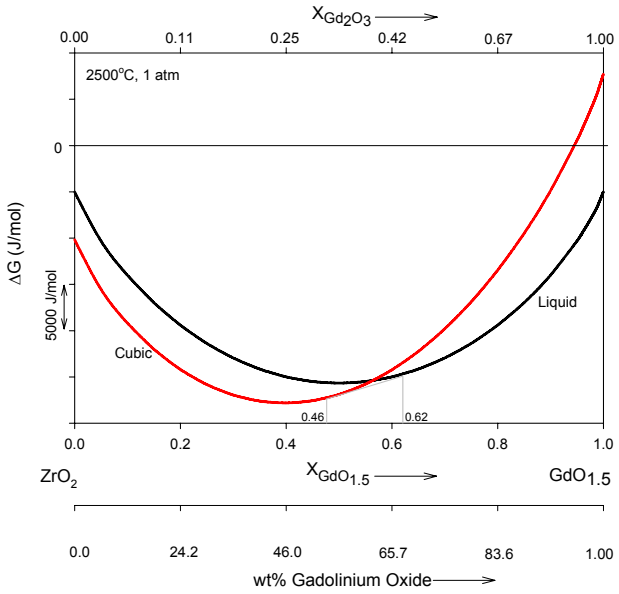


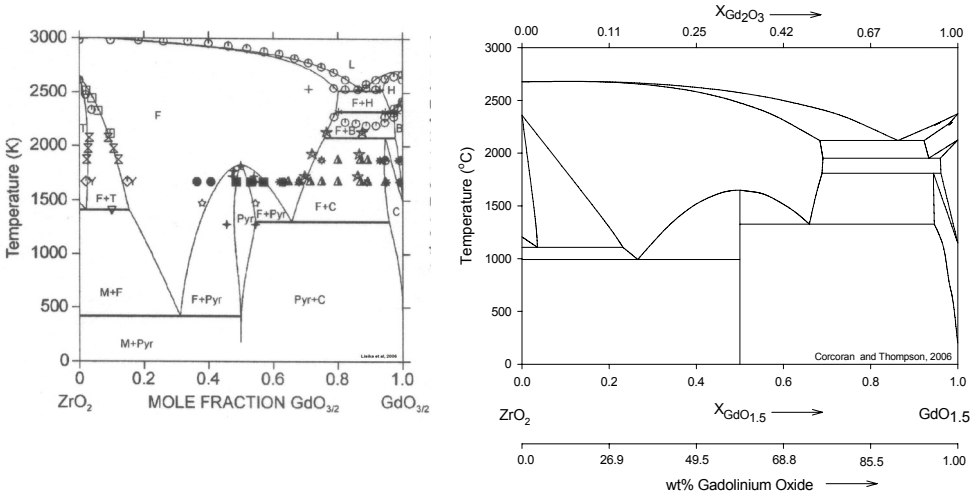
Figure 4. Gibbs energy curves for cubic and liquid phases at 2500°C and 1 atm.

By utilizing the methodology of Gibbs energy minimization, the phase with the lower Gibbs energy at a given temperature and composition is the phase that is most stable [2]. However, between the line of common tangency running from 0.46 to 0.62 $X_{GdO_{1.5}}$, two phases are more stable then either one separately. Accordingly, represented in Figure 3 (at 2500°C):

- between 0 and 0.46 $X_{GdO_{1.5}}$ cubic is most stable;
- between 0.62 and 1 ($X_{GdO_{1.5}}$) liquid is most stable;
- between 0.46 and 0.62 ($X_{GdO_{1.5}}$) a mechanical mixture of both liquid and cubic is most stable (two phase region).

6.1 ZrO_2-$GdO_{1.5}$ Binary Phase Diagram

The thermodynamic methodology described above can be expanded to include all of the phases present in the binary system (these include: monoclinic, hexagonal, tetragonal, and bixbyite) and excess mixing parameters can be tuned to match the latest accepted version of the phase diagram. This approach does not preclude using measurements of the Gibbs energy of mixing or related properties but because this information is not currently available.

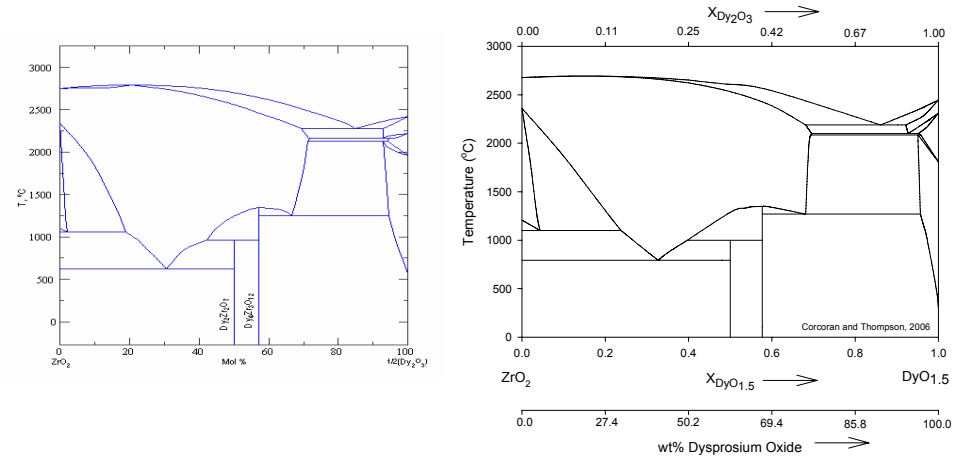


(a) **(b)**

Figure 5. (a) Recently proposed (2006) binary ZrO_2-$GdO_{1.5}$ phase diagram by Lakiza et al. Solid lines represent thermodynamic model. Data points represent experimental measurements [9]. (b) Thermodynamic binary model developed to match Lakiza et al.

6.2 ZrO_2-$DyO_{1.5}$ Binary Phase Diagram

The process applied to the ZrO_2-$GdO_{1.5}$ system can also be adapted to the ZrO_2-$DyO_{1.5}$ system. The major difference is that ZrO_2 and Dy_2O_3 can form two oxide compounds whereas ZrO_2-Gd_2O_3 forms only one.



(a) **(b)**

Figure 6. (a)Yokokawa et al. binary phase diagram for ZrO_2 and ½ Dy_2O_3 appearing in the ACeRs-NIST v3.0 Database. (Note: ½ Dy_2O_3 =$DyO_{1.5}$) [8]. (b) Thermodynamic binary model developed to match Yokokawa et al.

7 Estimated Phase Equilibrium in Ternary Systems

One system considered for the central element material is the ternary zirconia-gadolinia-dysprosia system. This ternary phase system is the integration of the binary phase diagrams for ZrO_2-$GdO_{1.5}$, ZrO_2-$DyO_{1.5}$ with ideal mixing assumed for the various phases in the gadolinia and dyprosia mixtures.

The estimated Gibbs energy at ternary composition point *t* (Figure 7) includes contributions from ideal mixing and excess terms. The ideal term is expanded to be of the form [2]:

$$\Delta G_{mix}^{ideal} = X_{ZrO_2} RT \ln(X_{ZrO_2}) + X_{GdO_{1.5}} RT \ln(X_{GdO_{1.5}}) + X_{DyO_{1.5}} RT \ln(X_{DyO_{1.5}}) \quad (6)$$

For any of the solution phases the excess term is an interpolation from the three binary sub-systems as follows [2,10,11]:

$$G_T^E = \left(\frac{X_{GdO_{1.5}}}{X_{GdO_{1.5}} + X_{DyO_{1.5}}} \right) G_a^E + \left(\frac{X_{DyO_{1.5}}}{X_{GdO_{1.5}} + X_{DyO_{1.5}}} \right) G_b^E + (X_{GdO_{1.5}} + X_{DyO_{1.5}})^2 G_c^E \quad (7)$$

To numerically illustrate, the Gibbs energy (ideal and excess) for the cubic phase can be calculated at 1800°C for points *a*, *b*, *c*, and *t* on Figure 7. These are shown in Table 2.

Table 2. Computed Gibbs energy of mixing for ZrO_2-$GdO_{1.5}$-$DyO_{1.5}$ in the cubic phase present at X_{ZrO_2}=0.40, $X_{GdO_{1.5}}$=0.20 and $X_{DyO_{1.5}}$=0.40 (1800°C). See Figure 7.

Point	ΔG_{mix}^{ideal} (kJ/mol)	G_T^E (kJ/mol)	ΔG_{mix} (kJ/mol)
a	-208.54	-6.15	-214.69
b	-211.38	-6.85	-218.23
c	-435.08	0.00	-435.08
t	-215.46	-6.62	-222.08

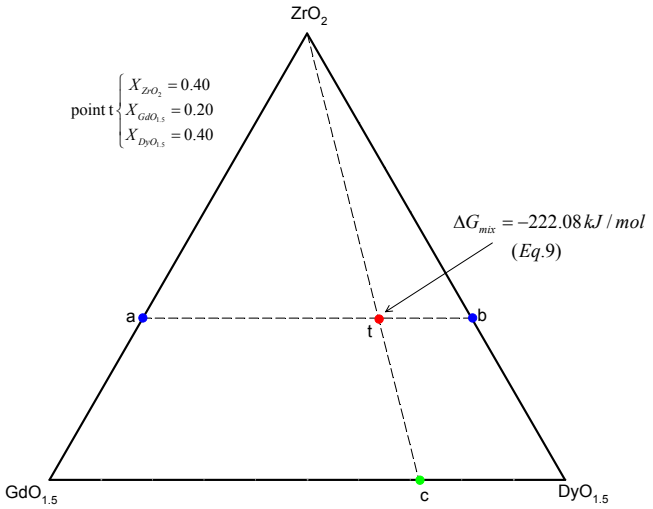


Figure 7. Toop interpolation [11] scheme for Gibbs energy of mixing for the cubic phase at 1800°C. Gibbs energies at *a*, *b*, *c*, and *t* appear in Table 7.

The Gibbs energy can be calculated in the same manner for other ternary phases liquid, monoclinic (Ln rich), hexagonal, tetragonal and bixbyite. At point *t* in Figure 7, the cubic phase has the lowest Gibbs energy (Table 3) and corresponds with the phase field placement in Figure 8.

Table 3. Gibbs Energy of mixing for all phases present at X_{ZrO_2}=0.4, $X_{GdO_{1.5}}$=0.20 and $X_{DyO_{1.5}}$=0.40 (1800°C). Note: the lowest Gibbs energy corresponds to the cubic phase which is consistent with the phase field placement at 1800°C in Figure 8.

Phase	ΔG_{mix} (kJ/mol)
Cubic	-222.08
Tetragonal	-216.08
Liquid	-212.54
Monoclinic	-213.62
Bixbyite	-214.38
Hexagonal	-215.46

The computed ternary isothermal sections for the ZrO_2-$GdO_{1.5}$-$DyO_{1.5}$ system at 1800 and 900°C are shown in Figure 8 and Figure 9. These computations are based on the same methodology of Gibbs energy minimizations (used to develop the binary phase diagrams). When ternary Gibbs energy surfaces intersect, implying that ternary phases may co-exist, the compositions for the co-existing phases (ends of tie-lines) can be established in concept by geometrically finding common tangent points associated with a doubly rolling tangent plane.

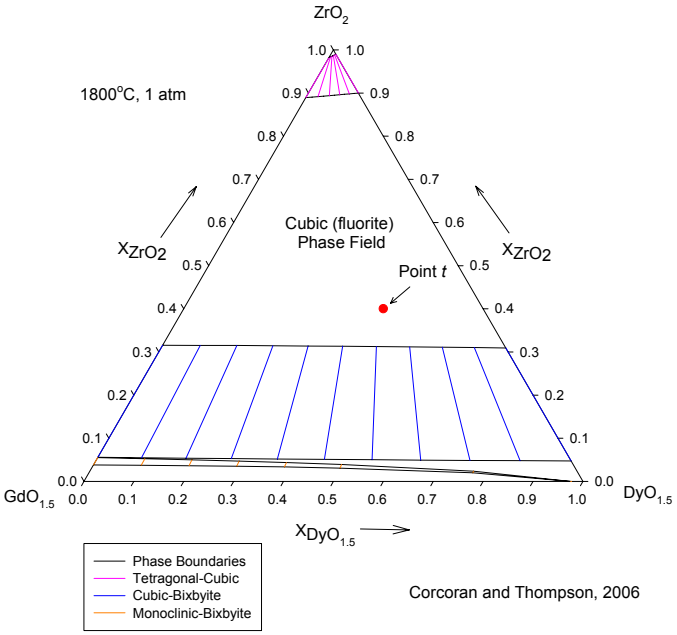


Figure 8. Computed ternary phase diagram for ZrO_2-$GdO_{1.5}$-$DyO_{1.5}$ systems at 1800°C.

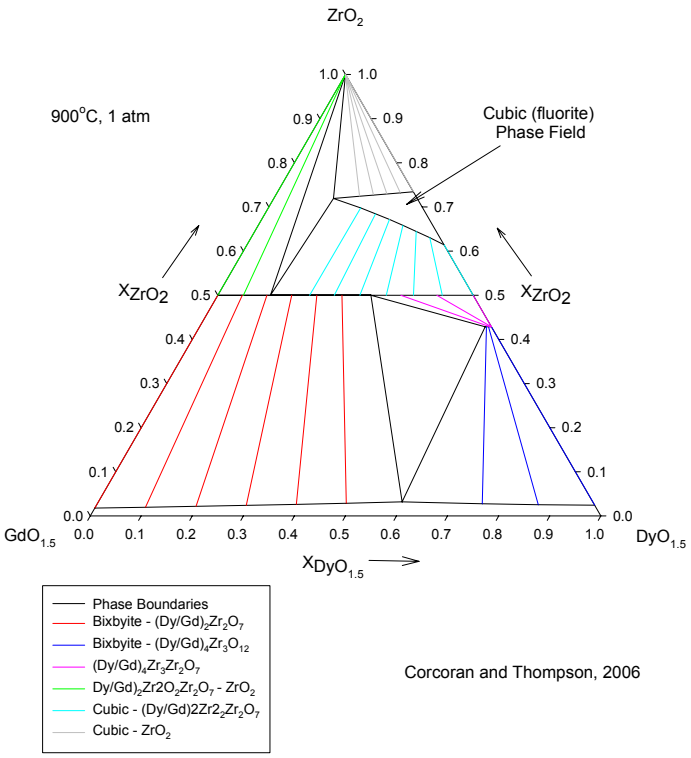
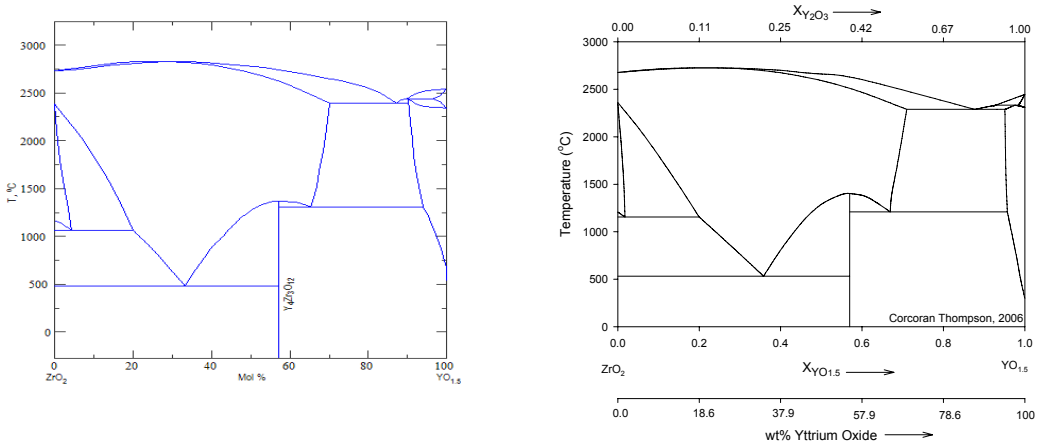


Figure 9. Computed ternary phase diagram for ZrO_2-$GdO_{1.5}$-$DyO_{1.5}$ systems at 900°C.

8 Estimated Phase Equilibrium in the ZrO_2-$YO_{1.5}$-$GdO_{1.5}$-$DyO_{1.5}$ (Quaternary) System

The quaternary integration scheme is much the same as the ternary system (discussed above) with the addition of the zirconia-yttria binary phase diagram (shown in Figure 10).



(a) **(b)**

Figure 10. (a)Yokokawa et al. binary phase diagram for ZrO_2 and ½ Y_2O_3 appearing in the ACeRs-NIST v3.0 Database. (Note: ½ Y_2O_3 =$YO_{1.5}$) [8]. (b) Thermodynamic binary model developed to match Yokokawa et al.

The Gibbs energy equations for the quaternary multi-components system are shown below; the ideal term is expanded to [2]:

$$\Delta G_{mix}^{ideal} = X_{ZrO_2} RT \ln(X_{ZrO_2}) + X_{GdO_{1.5}} RT \ln(X_{GdO_{1.5}}) + X_{DyO_{1.5}} RT \ln(X_{DyO_{1.5}}) + X_{YO_{1.5}} RT \ln(X_{YO_{1.5}}) \quad (8)$$

The Toop interpolation for the excess term is expanded for the four binary sub-systems* [2]:

$$\Delta G_T^E = \left(\frac{X_{GdO_{1.5}}}{X_{GdO_{1.5}} + X_{DyO_{1.5}} + X_{YO_{1.5}}}\right) G^E_{ZrO_2-GdO_{1.5}} + \left(\frac{X_{DyO_{1.5}}}{X_{GdO_{1.5}} + X_{DyO_{1.5}} + X_{YO_{1.5}}}\right) G^E_{ZrO_2-DyO_{1.5}} + \left(\frac{X_{YO_{1.5}}}{X_{GdO_{1.5}} + X_{DyO_{1.5}} + X_{YO_{1.5}}}\right) G^E_{ZrO_2-YO_{1.5}} + (X_{GdO_{1.5}} + X_{DyO_{1.5}} + X_{YO_{1.5}})^2 G_{GdO_{1.5}-DyO_{1.5}-YO_{1.5}} \quad (9)$$

It is not possible to graphically represent a quaternary system effectively in conventional phase diagram format. Therefore, the phases and their proportions present at a particular composition over a range of temperatures are represented on a bar graph (in which the oxides of Y, Gd, and Dy are lumped together as Ln in the resultant phases). As seen in Figure 11, if this mixture is sintered at 1200°C long enough, a homogeneous cubic phase would form. At reactor operational conditions, thought to be approximately 300-600°C, the thermodynamic model predicts that the sintered cubic compound would become a mixture of monoclinic and the stoichiometric compounds† (as seen in Figure 11).

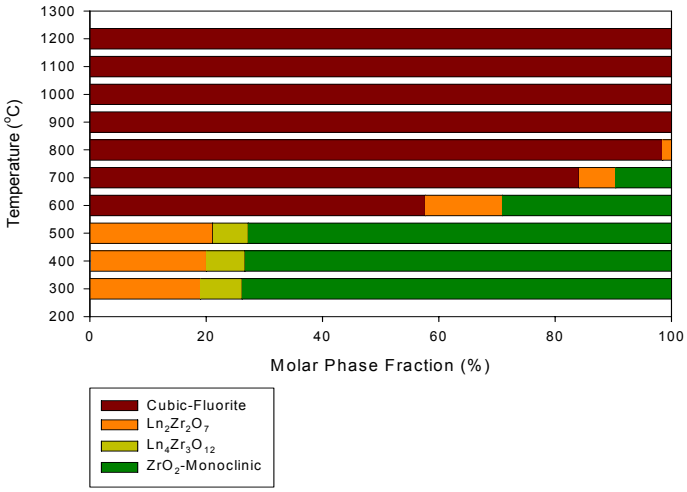
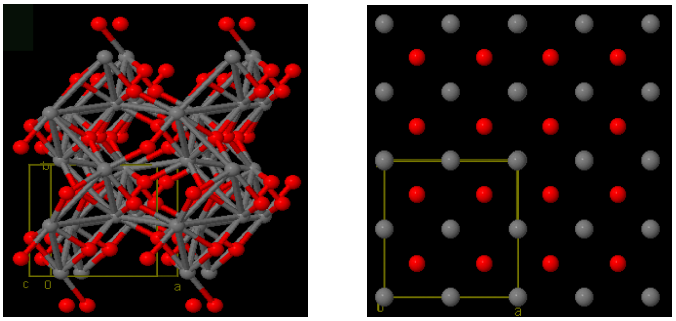


Figure 11. Phase compositional bar graph in mole percent. For an 80 mol% ZrO_2, 6.67 mol% $YO_{1.5}$, 6.67 mol% $GdO_{1.5}$, and 6.67 mol% $DyO_{1.5}$.

If this change in phase occurs, it is expected that a volume increase of the material might occur since the monoclinic structure of the pure ZrO_2 (predicted to form) is not as densely packed as the cubic structure (Figure 12) from which it was formed.

* Three binary systems discussed above and one system ($GdO_{1.5}$-$DyO_{1.5}$-$YO_{1.5}$) which assume ideal mixing between the component lanthanide oxides in each of the possible phases

† $Ln_2Zr_2O_7$ and $Ln_4Zr_3O_{12}$ (are near cubic structures)



(a) (b)

Figure 12. (a) Structural composition of monoclinic zirconia (baddeleyite) [12] versus (b) Structural composition of cubic fluorite zirconia [13]. Zr^{4+} ions are in red; O^{2-} ions in grey.

It is important to note that the thermodynamic model predicts what is most stable at a given temperature; it does not predict the rate at which the necessary phase changes occur. Currently an investigation using high temperature X-Ray Diffraction (XRD) on mixed oxide sample(s)‡ is underway. This work and related measurements of the thermal expansion coefficient of the cubic (fluorite) solid solution by lattice constant shift will be discussed during the presentation.

9 Summary

This work describes thermodynamic models for the binary systems of zirconia – gadolinia, zirconia – dysprosia, and zirconia – yttria. These were incorporated into ternary and quaternary systems using the Toop interpolation. Phase stabilities as a function of temperature and lanthanide composition are discussed in relation to reactor conditions.

10 Acknowledgements

The author recognizes and thanks AECL-CRL, especially, P. Boczar, L. Dickson, Z. He, R. Verrall, J. Mouris, and H. Hamilton for their continued collaboration and support which have made this project possible. The author also recognizes the continued support of Dr. W. T. Thompson and Dr. B. J. Lewis; their insight and guidance have been extremely valuable to this work.

11 References

1. P. Boczar, "CANDU Fuel Design Process", *9th International CNS Conference on CANDU Fuel. Belleville, Ontario, Canada. September 18-21,(2005).*
2. A. Pelton, W. T. Thompson, "Phase Diagrams", *Progress in Solid State Chemistry,* **10**, Part 3, 119-155, (1975).
3. G. Adachi, Z. C. Kang, *Binary Rare Earth Oxides*, Chapter 1, Kluwer Academic Publishing (2004).
4. K. Branderburg, "Diamond 3.1a Crystallographic Software*". Crystal Impact GbR. Bonn, Germany. (1997-2005).*
5. W. B. Pearson, *A Handbook of Lattice Spacings and Structures of Metals and Alloys*, Pergamon, **1**,(1958), **2**,(1967).
6. K. Clausen, W. Hayes, J.E. MacDonald, P. Schnabel, M.T. Hutchings, "Inorganic Crystal Structure Database" *(ICSD) ICSD-77701.*
7. C. H. P. Lupis, *Chemical Thermodynamics of Materials*, Chapters 1-4, North-Holland, (1983).
8. H. Yokokawa, N. Sakai, T. Kawada, and M. Dokiya, "Phase diagram calculations for ZrO_2 based ceramics: thermodynamic regularities in zirconate formation and solubilities of transition metal oxides", *5th International Conference in Science and Technology. Melbourne, Australia, August 16-21, 59-68,(1992).*
9. S. Lakiza, O. Fabrichnaya. C. Wang, M. Zinkevich, F. Aldinger., "Phase Diagrams of the ZrO_2-Gd_2O_3-Al_2O_3 System", *Journal of the European Ceramic Society,* ***26***, 233-246,(2006).
10. C. W. Bale, A. D. Pelton, W. T. Thompson, "Facility for the Analysis of Chemical Thermodynamics". *Ecole Polytechnique de Montréal,(2002).*
11. G.W. Toop, *Trans. Met. Soc. AIME,* ***233****, 850,(1965).*
12. J. D. McCullough, K. N. Trueblood, "The crystal structure of baddeleyite (monoclinic ZrO_2)", *Acta Crystallographica* **12** 507-511,(1959)
13. S. Speziale, T. S. Duffy, "Single-crystal elastic constants of fluorite (CaF2) to 9.3 GPa". *Physics and Chemistry of Minerals* **29** 465-472,(2002).

‡ Samples provided by AECL-CRL